STIFS: Spatio-Temporal Input Frame Selection for Learning-based Video Super-Resolution Models

Arbind Agrahari Baniya[a], Tsz-Kwan Lee[b], Peter W. Eklund[c] and Sunil Aryal[d]
School of IT, Deakin University, Geelong, VIC, Australia

Keywords: High Definition Video, Image Analysis, Image Quality, Video Signal Processing, Super-resolution.

Abstract: Deep learning Video Super-Resolution (VSR) methods rely on learning spatio-temporal correlations between a target frame and its neighbouring frames in a given temporal radius to generate a high-resolution output. Among recent VSR models, a sliding window mechanism is popularly adopted by picking a fixed number of consecutive frames as neighbouring frames for a given target frame. This results in a single frame being used multiple times in the input space during the super-resolution process. Moreover, the approach of adopting the fixed consecutive frames directly does not allow deep learning models to learn the full extent of spatio-temporal inter-dependencies between a target frame and its neighbours along a video sequence. To mitigate these issues, this paper proposes a Spatio-Temporal Input Frame Selection (STIFS) algorithm based on image analysis to adaptively select the neighbouring frame(s) based on the spatio-temporal context dynamics with respect to the target frame. STIFS is first-ever dynamic selection mechanism proposed for VSR methods. It aims to enable VSR models to better learn spatio-temporal correlations in a given temporal radius and consequently maximise the quality of the high-definition output. The proposed STIFS algorithm achieved remarkable PSNR improvements in the high-resolution output for VSR models on benchmark datasets.

1 INTRODUCTION

Super-Resolution for generating high-resolution visuals from low-resolution inputs is a classic problem in computer vision domain. Its initial solution was provided by Image Super-Resolution (ISR) which only utilises spatial information of a single image or multiple discrete images to produce fundamental visual quality improvement (Wang et al., 2020; Arefin et al., 2020). Extending the target resolving subject from image to video signals, applying the super-resolution approaches used in conventional ISR to Video Super-Resolution (VSR) fails to capture the unique temporal information present in videos (Liang et al., 2020; Liu et al., 2021). VSR aims to adopt several temporally correlated low-resolution frames within a video sequence to super-resolve the frame series. The cross-consideration of spatial and temporal dimensions across multiple input frames has induced a highly non-linear multi-dimensional problem to tackle.

In recent years, Deep Neural Networks (DNN) have been widely adopted in the VSR domain to leverage highly non-linear multi-dimensional characteristics and features in the input video frames and have shown some promising results (Liu et al., 2020). Other learning-based VSR approaches (Haris et al., 2019; Wang et al., 2019b; Jo et al., 2018; Bao et al., 2021; Tian et al., 2020; Isobe et al., 2020b; Chan et al., 2021; Isobe et al., 2020a) utilise temporal information in a video as a learning feature followed by stages of frame alignment and fusion to reconstruct and up-sample the resultant pixels. However, their commonly adopted frame alignment techniques, traditional Motion Estimation and Motion Compensation (MEMC) approach using optical flow and warping (Chan et al., 2021), or modern machine learning technologies such as deformable convolution (Dai et al., 2017) may not effectively align multiple frames correctly for accurate fusion and reconstruction (Liu et al., 2020). Therefore, 2D/3D and recurrent convolutions have been used to learn the inter-frame correlation without any implicit or explicit frame alignment.

To reveal inter-frame correlation along a video se-

[a] https://orcid.org/0000-0002-9359-6506
[b] https://orcid.org/0000-0003-4176-2215
[c] https://orcid.org/0000-0003-2313-8603
[d] https://orcid.org/0000-0002-6639-6824

Agrahari Baniya, A., Lee, T., Eklund, P. and Aryal, S.
STIFS: Spatio-Temporal Input Frame Selection for Learning-based Video Super-Resolution Models.
DOI: 10.5220/0011339900003289
In *Proceedings of the 19th International Conference on Signal Processing and Multimedia Applications (SIGMAP 2022)*, pages 48-58
ISBN: 978-989-758-591-3; ISSN: 2184-9471

quence without any implicit or explicit frame alignment, the input frames adopted to be learned is commonly based on a sliding window mechanism including n consecutive frames from either past and/or future timestamps to the target frame (Sajjadi et al., 2018). Most VSR models using a sliding-window mechanism treat all neighbouring input frames as equally important without rank or selection. However, each neighbouring frame in a sliding window may express a different correlation because of the context changes across the time domain. Thus, a fixed selection of n consecutive frame(s) from the target frame in a sliding window may not be optimal for learning spatio-temporal correlation (Wang et al., 2019b).

In this work we propose to address these gaps with three-fold contributions highlighted as follows:

1. To leverage a VSR result from an optimal input space, we propose a novel pre-processing technique which adaptively ranks and selects the neighbouring frames from bidirectional temporal dimensions to be included in the sliding window input space based on a spatio-temporal ranking algorithm, rather than simply selecting the nearest n consecutive frames from the target frame.
2. The proposed Spatio-Temporal Input Frame Selection (STIFS) algorithm induces a strategic correlation-based discrepancy among the neighbouring frames to enable selection of the most highly correlated reference frames from bidirectional temporal dimensions for super-resolving the target frame.
3. Finally, this work explores the impact and effectiveness of applying an input selection algorithm for machine learning based VSR model.

To our knowledge, this is the first work of its kind that introduces an adaptive selection algorithm with the objective of optimising the input space to aid VSR models to learn better spatio-temporal correlations in VSR and consequently improve the quality of high-resolution outputs.

2 BACKGROUND

2.1 Trade-off with and without Frame Alignment in VSR

Using frame alignment in VSR, MEMC (Haris et al., 2019; Bao et al., 2021; Haris et al., 2020; Xue et al., 2019) remains challenging, particularly when inter-frame motion is large, or when there is luminance variance across frames (Hung et al., 2019). Alternatively, deformable convolutions proposed by Dai *et al.* (Dai et al., 2017) has been used for frame alignment by enhancing DNN's capacity to model the transformation of geometric variations of objects. Although deformable convolution is tolerant to variance in luminance or motion, it involves higher computational overhead (Tian et al., 2020; Wang et al., 2019a; Wang et al., 2019b). Recently, more VSR methods have been proposing to not rely on frame alignment techniques to alleviate the above-mentioned limitations. These methods promote 2D convolution (Lucas et al., 2019), 3D convolution (Jo et al., 2018; Kim et al., 2018), or Recurrent Convolution Network (RCN) (Isobe et al., 2020c; Zhu et al., 2019) to exploit spatial or spatio-temporal information in a video.

Most VSR models simply use a fixed set of n consecutive frames for super-resolution a whole video, some recent methods have introduced variations of the learning network architecture to extract different features from the given n consecutive frames attempting to capture the unique temporal characteristics between video frames. Enhanced Deformable Convolution Networks (EDVR) (Wang et al., 2019b) makes use of a Temporal-Spatial Attention (TSA) mechanism where convolution-based similarity distance is used to generate temporal attention maps in element-wise multiplication with the original feature maps of the frame and compute a spatial attention mask by a fusion process. Even incorporated with such complex components like TSA, the information feed in via input frames to these models remains the same. This implies that the learning by the model is only relied on the same inputs to map low-resolution frames to a higher resolution output, even the operations applied to extract features from the input might vary.

Based on the literature, it is manifest that it lacks mechanism to effectively select the input frames for either alignment-based models or non-alignment based models. Non-frame alignment models suffer more from redundancy in the input space, with the exception of RCN-based models, which commonly use one consecutive frame in addition to the target frame and the hidden state propagated from super-resolving frames from past timestamps. Two of the non-frame alignment-based methods are VSRResFeatGAN (Lucas et al., 2019) and Dynamic Upsampling Filters (DUF) (Jo et al., 2018), which use 2D and 3D convolution respectively. Both methods make use of a sliding window mechanism to select n frames from both past and future temporal dimensions and rely on 2D convolution to extract the spatial correlation, and 3D convolution to extract the spatio-temporal correlation respectively. However, such an approach has still

led these models to use identical frames repeatedly, compromising their super-resolution performance as a result.

2.2 VSR Challenges

IconVSR (Chan et al., 2021) harnessed the sequential modelling ability of bidirectional recurrent neural networks in combination with MEMC to obtain PSNR improvement of only 0.03 dB over the previously best performing model, EDVR (Wang et al., 2019b) on Vimeo90k test set. This exemplifies the challenges in improving performance of existing VSR models. Interesting to mention is the extent of the changes made to the model to obtain this meagre improvement. Similarly, despite the complexity of the model proposed, the recent BasicVSR model is only able to improve the PSNR on Vid4 by 0.04 dB compared to the previously best performing model Recurrent Structure-Detail Network (RSDN) (Isobe et al., 2020a). RSDN in turn was only able to improve the super-resolution outcome on Vid4, in PSNR terms, by 0.07 dB compared to the EDVR model, the best performing model preceding RSDN. Although the evaluation of new VSR models is beyond the scope of this paper, our intention with this discussion is to demonstrate the fierce competition in VSR research space, and the relatively small gains, achieved via modelling and addressing the complex problem of video super-resolution.

Our literature study concludes that, although limited attempts have been made to treat frames at different timestamps differently in some frame alignment-based methods, no work has been proposed to effectively select the input space itself in both categories of models, despite the hypothesis that such an approach will likely decrease redundancy in the feature space, and may achieve improved super-resolution outcomes, especially for non-frame-alignment based VSR models. At the same time, it is hypothesised that selecting the most relevant input space will improve VSR results at lower computational cost compared to models which add learnable parameters to differentiate between input frames. The remainder of this paper is organised as follows. The design of our proposed algorithm for selecting frames in the input space is presented in Section 3, the methodology is explained in Section 4, the results are evaluated in Section 5, Conclusions are drawn in Section 6.

3 PROPOSED ALGORITHM AND ITS ANALYSIS

3.1 The STIFS Algorithm

To mitigate the shortcomings of current VSR models, our novel Spatio-Temporal Input Frame Selection (STIFS) algorithm makes use of the frame-wise spatio-temporal correlation between neighbouring frames and the target frame to capture their relationship in the input space to a VSR network. The frame-wise spatio-temporal correlation comprises spatial difference and temporal difference between frames. To compute the spatial difference, we make use of Mean Pixel Value Difference (MPVD) between the target frame F_t and the neighbouring frame F_{t+i}, where $i \in \{\pm\ 1, \cdots, \pm\ 2s+1\}$, $(2s+1$ is the number of frames in the selection window), defined as,

$$MPVD(F_t, F_{t+i}) = \frac{1}{h \times w} \sum_{j=1}^{h \times w} \|p_j(F_t) - p_j(F_{t+i})\| \tag{1}$$

where h and w are the height and width of the frames in terms of pixels, respectively; $p_j(\cdot)$ is the value of j^{th} pixel of a given frame.

The temporal component of the spatio-temporal correlation is the Temporal Distance (TD) between a target frame F_t and neighbour F_{t+i} calculated as,

$$TD(F_t, F_{t+i}) = \|i\|. \tag{2}$$

The rank score for each frame F_{t+i} in the neighbouring space of target frame F_t is then computed as,

$$r(F_{t+i}) = \frac{MPVD(F_t, F_{t+i})}{TD(F_t, F_{t+i})}. \tag{3}$$

The STIFS algorithm then uses the rank scores of neighbouring frames to select s frames from $2s+1$ frames, either side of the target frame F_t (past and future), resulting in a total of $2s+1$ (including $2s$ neighbours and F_t itself) frames as input to super-resolve the target frame F_t. The overall algorithm for the frame selection to an input space of a VSR model for a given video sequence with the total number of frames f, where each frame is of size $h \times w$, is presented in Algorithm 1. Based on our proposed STIFS Algorithm 1, the selection is repeated for each target frame F_t in a video sequence, finally giving an input space of size $2s+1$ for each target frame F_t. It selects neighbouring frames by ranking them while capturing both spatial and temporal correlation between F_t and each neighbouring frame $F_t + i$. The result is an

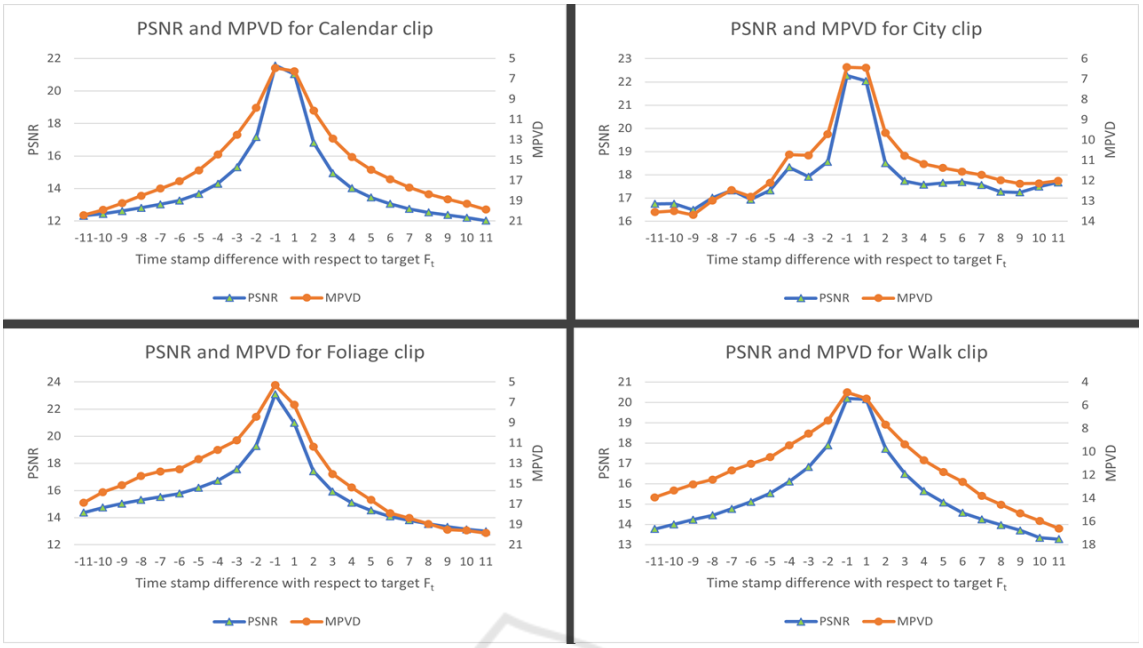

(a) PSNR and MPVD correlation in 4 clips of Vid4 Dataset

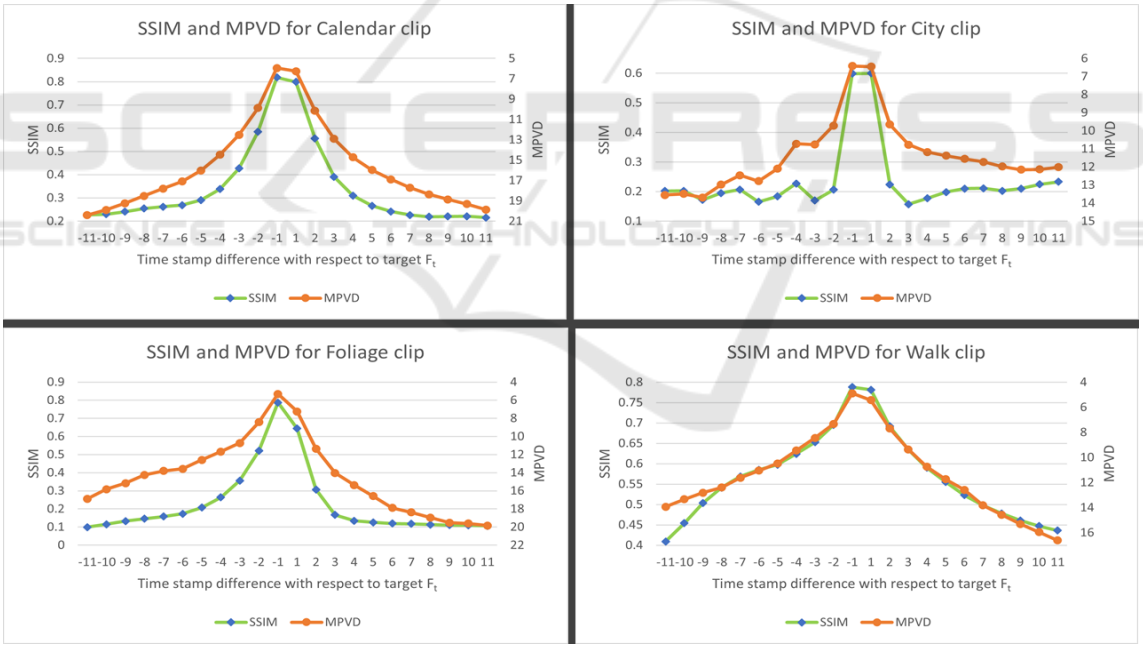

(b) SSIM and MPVD correlation in 4 clips of Vid4 Dataset

Figure 1: PSNR, SSIM and MPVD Correlation between target frame F_t, where $t = 12$ and its 11 neighbours in each temporal direction in 4 clips of the benchmark Vid4 Dataset.

input space to a VSR model is formed by appending the selected frames with higher spatial and temporal correlation with respect to the target frame.

3.2 Analysis of Selection Measures in STIFS

To understand the intuition behind using MPVD based selection, we perform frame-to-frame compar-

Algorithm 1: STIFS Algorithm.

Result: Sliding window of size $2s+1$ frames for each target frame F_t
Initialisation: future_score = [], past_score = [], input = [] ;
$i \leftarrow 1$;
while $i < 2s+1$ **do**
  $MPVD(F_t, F_{t+i})$ using eqn. (1);
  $TD(F_t, F_{t+i})$ using eqn. (2);
  $r(F_{t+i})$ using eqn. (3);
  future_score.append($r(F_{t+i})$);
  $i = i+1$;
future_score.sort_descending();
$i \leftarrow -1$;
while $i > -(2s+1)$ **do**
  $MPVD(F_t, F_{t+i})$ using eqn. (1);
  $TD(F_t, F_{t+i})$ using eqn. (2) ;
  $r(F_{t+i})$ using eqn. (3);
  past_score.append($r(F_{t+i})$);
  $i = i-1$;
past_score.sort_descending();
$i \leftarrow -1$;
while $i > -(2s+1)$ **do**
  if $r(F_{t+i})$ *in past_score[:s]* **then**
    input.append(F_{t+i});
  $i = i-1$;
input.append(F_t);
$i \leftarrow 1$;
while $i < 2s+1$ **do**
  if $r(F_{t+i})$ *in future_score[:s]* **then**
    input.append(F_{t+i});
  $i = i+1$;

ison between example target frames and its neighbours. Well-known image/frame comparison matrices namely PSNR and SSIM are computed between a target frame F_t and its $2s+1$ neighbours in each temporal direction for all the four clips of the Vid4 dataset. For this analysis we consider F_t, where $t = 12$ as target frame, and its 11 neighbours in each temporal direction. From the graphs shown in Fig. 1a and Fig. 1b it is evident that MPVD is highly correlated with both PSNR and SSIM, justifying the ability of MPVD to capture similarity/difference between frames, and therefore for it to be used as a selection metric.

However, unlike PSNR and SSIM, MPVD has significantly lower computation cost resulting in less time taken to compute rank score as shown in Table 1. Since the selection of neighbouring frames for a given target frame in VSR is to be done repeatedly using a sliding window over the entire video, it is crucial to consider the cost associated with such selection. It is evident from Table 1 that the time taken to compute rank score is about 83% less on average compared to

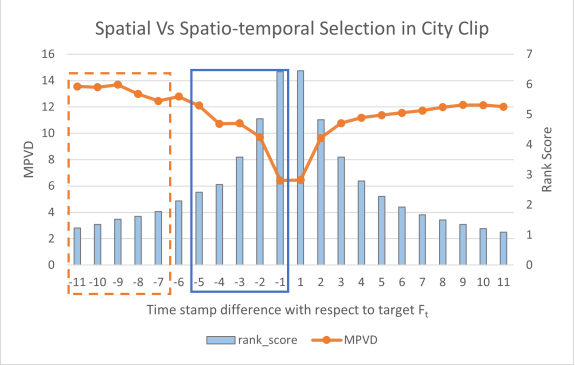

Figure 2: Comparison between spatial and spatio-temporal selection. The dashed bounding box represents frame selection based on spatial metric (MPVD) alone. The solid bounding box represents frame selection based on spatio-temporal metric (MPVD/TD).

PSNR computation for the same number of frames, making rank score the most suitable ranking measure for STIFS.

Table 1: Time taken in seconds to compute PSNR, SSIM and Rank Score between target frame $F_t, t = 12$ and its 11 neighbours in each temporal direction in 4 clips of Vid4 Dataset.

Clip Name	PSNR Time(s)	SSIM Time(s)	Rank Score Time(s)	Computational Reduction(%) by Rank Score over PSNR
Calendar	0.0130	0.6173	0.0027	79.32
City	0.0136	0.5959	0.0023	83.09
Foliage	0.0113	0.4599	0.0016	85.84
Walk	0.0119	0.4832	0.0018	84.87
Avg.	0.0125	0.5391	0.0021	83.28

Furthermore, consideration of only a spatial comparison between frames for selection does not consider the actual spatio-temporal inter-dependencies among video frames. As shown in Fig. 2, if we are to consider selection of $s = 5$ out of $2s+1 = 11$ past frames with reference to target frame F_t, where $t = 12$ for the City clip, based on spatial metric MPVD only, the most distant 5 frames from the target frame are selected because they exhibit the largest spatial differences, as highlighted by dotted bounding box in Fig. 2. However, when Temporal Distance (TD) is considered, the most distant frames rank lowest despite having the largest MPVD with F_t and thus, the nearest 5 frames are selected, as highlighted by solid bounding box in Fig. 2. Considering spatial dimension alone inverts the VSR to MISR, which is undesirable. To capture true spatio-temporal interdependence between the target and its neighbours both spatial and temporal dimensions must be considered.

4 METHODOLOGY

We apply the proposed STIFS algorithm to establish a highly correlated input space to super-resolve video clips in three widely used benchmark VSR datasets, namely Vid4 (Liu and Sun, 2013), SPMCS (Tao et al., 2017) and Vimeo90k (Xue et al., 2019). For the purpose of super-resolution, we have considered three different VSR models that include both frame-alignment and non-frame alignment-based methods, to show the diverse applicability of the proposed algorithm. Two out of the three models are non-frame alignment models (designed by us) for simulation of real-world VSR models based on 2D convolutions. The two simulation models differ in the number of input frames used to show the different impact of STIFS when selecting from a smaller or larger temporal radius. The third model is the RBPN model (Haris et al., 2019), widely used for comparison in the VSR literature since 2019, as it was one of the best performing models in benchmark VSR competition NTIRE 2019 (Nah et al., 2019). The experimentation on each of these models varies in terms of the sliding window size and the deep learning model architecture used in order to show different emergent features in training and testing.

4.1 Simulation Models

The first VSR model (Simulation Model-1) is constructed with 2D convolutions with residual blocks and is shown in Fig. 3. It uses three frame inputs to super resolve a frame from its low-resolution frame F_t to the high-resolution result frame $F_t \times 4$. To do so, one of the three frames is selected in each direction based on the STIFS algorithm resulting in three low-resolution input frames including F_{t-1}, F_t, and F_{t+1}. These low-resolution input frames are generated by synthetically downsampling the ground-truth by $4\times$ using the bicubic downsampling technique. A 2D convolution operation with kernel of size 3×3 is then applied on each input frame resulting in 64 features from each input frame which are concatenated and subjected to another convolution with kernel of size 3×3. The 256 features extracted from the previous steps are passed through 5 residual blocks, where each residual block consists of a convolution operation with kernels of size 3×3, a Rectified Linear Unit (ReLU) layer, and an additional convolution operation identical to the first. The 256 features obtained after the final residual block is then subject to a convolution operation with kernels of size 3×3 to extract 48 features followed by pixel shuffling to perform a depth-to-space transformation. This is then concatenated with the $4\times$ bilinearly upsampled target input frame to obtain a $\times 4$ spatially super-resolved frame. This model is used to demonstrate the impact of the proposed STIFS algorithm with window size three, compared to the same VSR model without STIFS.

Fig. 4 illustrates the second VSR model for simulation (Simulation Model-2). Similar to Simulation Model-1, Simulation Model-2 adopts 2D convolutions with residual blocks but in this case with four neighbouring frames to super resolve the target frame F_t. To maintain a sliding window of five frames, two frames respectively from both temporal-directions are selected. The 2D convolution operation with kernel of size 3×3 is applied on each input frame resulting in 320 total feature maps, concatenated and subjected to another convolution with kernel of size 3×3 to extract 128 features. While the kernel size remains the same in each convolution for extracting the features, Simulation Model-2 involves larger input data volumes such that the following convolution processes are conducted by kernels with more nodes for the model to handle a higher complexity problem, compared to that in Fig. 3. As shown in Fig. 4, the feature maps are then passed through five residual blocks, each comprised of a convolution operation with 128 nodes followed by a ReLu layer and an additional convolution operation identical to the first. Afterwards, a convolution with 48 nodes is performed followed by pixel shuffling resulting in depth-to-space transformation. This is then concatenated with the $4\times$ bilinearly upsampled target input frame to obtain a $\times 4$ spatially super-resolved frame. This model is further used for verifying the impact of the proposed STIFS algorithm, compared to the same VSR model without the STIFS algorithm, with a sliding window of five frames.

For the purpose of training, the Vimeo90k (Xue et al., 2019) training set is used. Training is performed for 30 epochs each of the 4 models (the 2 models $\times$ 2 ways of selecting input). Each VSR simulation training uses L1 loss and Adam optimization. The batch size is fixed to 16 and a learning rate of 0.0001 is used. The code is implemented using PyTorch (Paszke et al., 2019). To test these models, the Vid4 dataset (Liu and Sun, 2013) and Vimeo90k test set (Wang et al., 2019b) is used and the performance of the each simulation model is measured in terms of Peak Signal-to-Noise Ratio (PSNR) and Structural Similarity Index Measure (SSIM) compared with (and without) the use of the proposed algorithm.

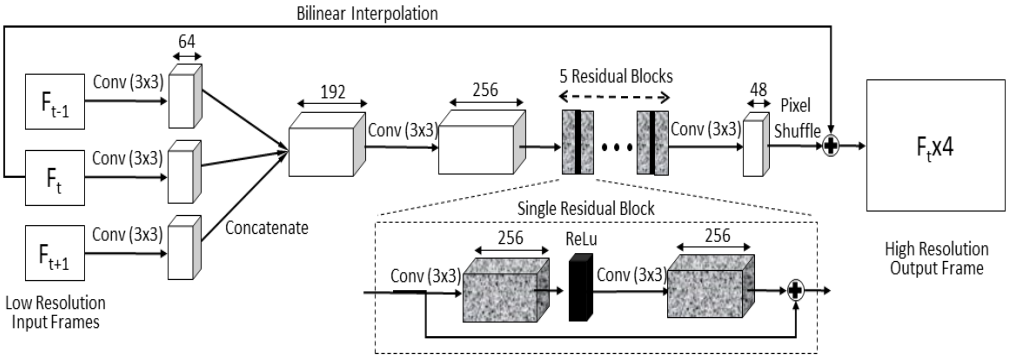

Figure 3: Simulation Model-1 architecture with three input frames.

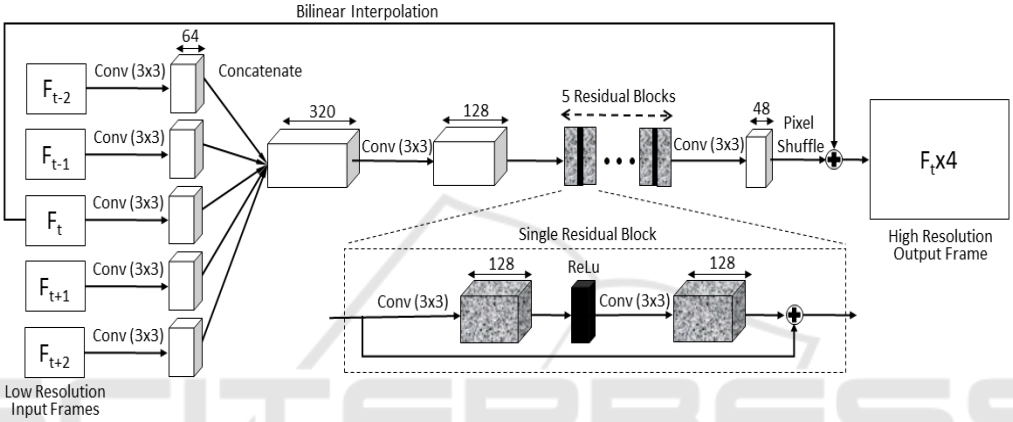

Figure 4: Simulation Model-2 architecture with five input frames.

4.2 RBPN Model

To evaluate the impact of the STIFS algorithm on benchmark methods, RBPN (Haris et al., 2019) was considered. Given that the model was originally trained using 7 frame sequences, in order to apply STIFS in the training phase we would need a training dataset with video sequences of at least $(2 \times 7) + 1 =$ 15 frames. However, the Vimeo90k dataset only contains 7 frames in each sequence, therefore we cannot perform the retraining of RBPN compared to the STIFS algorithm. Some more recent datasets, such as REDS (Nah et al., 2019), could be used but this would not allow us to conduct a fair baseline comparison with the published RBPN, trained on Vimeo90k, a much larger and diverse dataset compared to REDS. Nevertheless, we applied the STIFS algorithm during the test phase alone while using the pre-trained model published by the RBPN authors. The testing, with (and without) STIFS, is done on Vid4 and SPMCS datasets, as was done in the original RBPN work. For the purpose of testing, we selected 7 frames from 15 frames in consecutive sequence, including 3 past and 3 future frames along with one target frame. The model architecture and down-sampling of original frames is conducted in exactly the same way as the original RBPN work. For a fair comparison in the testing, we keep the sliding window to a fixed size of 7, as adopted in the original RBPN work.

5 EMPIRICAL EVALUATION RESULTS

In this paper, we evaluate the effectiveness of the proposed STIFS algorithm compared to a scenario without any selection mechanism in three different cases:

1. Simulation Model-1: the case with three frame inputs trained on Vimeo90k train set and tested on Vid4 and Vimeo90k test set. STIFS was applied at both train and test phase.
2. Simulation Model-2: the case with five frame inputs trained on Vimeo90k train set and tested on Vid4 and Vimeo90k test set. STIFS was applied at both train and test phase
3. A pre-trained RBPN model with seven frame inputs tested on SPMCS and Vid4 dataset. STIFS was applied at test phase only.

5.1 Simulation Model-1 with/without the STIFS Algorithm

Simulation Model-1 in Fig. 3 with three inputs is trained on the Vimeo90k and tested on the Vid4 dataset. As shown in Table 2, PSNR/SSIM is computed to evaluate the VSR outcome on each clip in the Vid4 dataset. This demonstrates that PSNR/SSIM results are improved when the STIFS algorithm is applied. The selection resulted in an overall PSNR/SSIM improvement of 0.22/0.01 on the Vid4 dataset which records the improvement resulting from applying the STIFS algorithm.

We further evaluated Simulation Model-1 on the Vimeo90k test set which contains 7,824 diverse clips from the real-world. Similar to the test we performed on Vid4, to super-resolve the fourth frame in the each of the septuplet clips, a three-frame sequence is used with one neighbour in each direction (along with the target frame). For no-selection, the third and fifth frames are used, as these are the immediate consecutive frames to the fourth frame. For selection, one out of the three frames is selected in each direction, based on the STIFS algorithm proposed. As shown in Table 2, even on a diverse test set like Vimeo90k, the use of the STIFS algorithm resulted in superior outcomes compared to no selection at all. The observed improvement is 0.05 dB for PSNR, a significant improvement in VSR research as discussed in Section 2.2.

5.2 Simulation Model-2 with/without the STIFS Algorithm

Simulation Model-2 is trained as depicted in Fig. 4 with five frame input sequences with (and without) the STIFS algorithm on the Vimeo90k train dataset. The trained models are tested on the Vid4 and Vimeo90k test datasets. It is important to note that Simulation Model-2 was trained to select 2 out of 3 frames in each temporal direction, because of 7 frames limitation of Vimeo90k clips.

As shown in Table 2, even with the training limitations, PSNR results are improved when the STIFS algorithm is used for each of the clips in Vid4. We observed a maximum improvement of up-to 0.95 dB and overall improvement of 0.34 dB when using the STIFS algorithm, compared to the baseline of no frame selection at all. On the other hand, the limitation of the temporal radius in the Vimeo90k dataset bounds the flexibility of input space selection even during the test phase. Thus, the improvement when using the STIFS algorithm on Vimeo90k test set could be even greater than what is reported but certainly not worse.

PSNR improvements of 0.22 dB and 0.34 dB are recorded on Vid4, using the STIFS algorithm with Simulation Model-1 and Simulation Model-2 respectively. Such improvements are considerable in the context of contemporary VSR research. This signifies improvement in the learning and modelling ability of a given VSR models when a spatio-temporal metric is used to select highly correlated frames in the input space. As discussed in Section 2.2, compared to the improvements resulted by multiple component changes in VSR models, the dominant methodology followed in VSR research, our simpler, yet effective, STIFS algorithm is able to improve super-resolution quality significantly over its none-selective counterpart.

5.3 RBPN with/without STIFS

Furthermore, to align our work with the VSR literature, we tested the STIFS algorithm on the RBPN model (Haris et al., 2019). We have tested the pre-trained model on the SPMCS and Vid4 datasets with (and without) the STIFS algorithm for our third evaluation scenario. The eight clips selected from the SPMCS dataset are identical to those provided in original RBPN evaluation. As observed in Table 3, PSNR is improved for 8 out of the 12 clips from SPMCS and Vid4 dataset. Even though the proposed STIFS algorithm was only applied at the test phase, it interestingly resulted in the observed PSNR improvement of 0.03dB in average. The original RBPN model is trained using 7 frames sliding window, with 3 consecutive frames used from each temporal direction (along with the target frame). While using the originally trained model, we made changes at the test phase. We performed two different tests, one with using 3 consecutive past and future neighbouring frames, i.e. no selection mechanism, and the other using our STIFS algorithm to select the 3 past, and future frames, from 7 frames in each direction. In both tests, the size of sliding window remains constant allowing us to use the originally trained RBPN with a 7-frame sliding window. We also observed improvement in PSNR outcomes for two clips, namely Calendar and City from the Vid4 dataset, when the STIFS algorithm is applied during the test phase alone, as observed in Table 3. This comparison, alongside RBPN, shows the effectiveness of STIFS even when applied only in the test phase. The improvement is most likely to be en-

[1]Due to the limitations of 7 frame clips in Vimeo90k dataset, 2 out of only available 3 frames were selected during both training and testing .

Table 2: Super-resolution results in terms of PSNR/SSIM on benchmark Vid4 and Vimeo90k test sets from VSR Simulation Model-1 (3 Frames Selection) and Simulation Model -2 (5 Frames Selection) with/without the proposed STIFS algorithm applied for both training and testing.

	3 Frames Selection		**5 Frames Selection**	
Clip Name	w STIFS	w/o STIFS	w STIFS	w/o STIFS
Calendar	**16.47/0.47**	15.98/0.46	**16.99/0.47**	16.04/0.46
City	**23.73/0.59**	23.67/0.59	**23.71/0.59**	23.61/0.59
Foliage	**21.45/0.52**	21.27/0.52	**21.07/0.50**	20.90/0.50
Walk	**20.56/0.73**	20.39/0.72	**20.08/0.71**	19.93/0.71
Avg. Vid4	**20.55/0.58**	20.33/0.57	**20.46/0.57**	20.12/0.57
Avg. Vimeo90k	**24.57/0.82**	24.52/0.82	**24.33/0.81**[1]	**24.33/0.81**

hanced further when STIFS is applied during training, as is evident from the outcomes from VSR Simulation Model-1 and Simulation Model-2, where the STIFS algorithm is used in both training as well as testing phases.

5.4 Visual Comparison

To further highlight the impact of the STIFS algorithm in the overall super-resolution task, we visually compare the outcomes from Simulation Model-1 on different video clips from Vid4. The images shown in Fig. 5 prove that the super-resolution outcomes, not only in spatial but also in temporal domain, significantly reduced artefacts and enhanced the finer details when applying the proposed STIFS algorithm compared no selection at all. It further demonstrates that the proposed STIFS algorithm is able to capture the spatio-temporal correction and alleviate the error propagation issue in VSR.

As highlighted with the red bounding box in each of Fig. 5a, 5b, 5c, and 5d, the STIFS algorithm is able to produce more correct pixels, with better defined shapes and boundaries of objects compared to video frames produced without using it. The difference is also evident with the better defined colours and significantly reduced artefacts in each frame. This provides further tangible, and easily identified, evidence of STIFS's effectiveness. Furthermore, it demonstrated that STIFS, as an input selection algorithm, is impactful and effective for achieving a better VSR outcomes.

Table 3: Super-resolution results in terms of PSNR on SPMCS and Vid4 from RBPN with/without the STIFS algorithm — applied during test phase only.

Clip Name	Dataset	w STIFS at test only	w/o STIFS at train+test
hitachi_isee5_001	SPMCS	26.21	**26.27**
hdclub_003_001	SPMCS	**21.95**	21.88
hk004_001	SPMCS	**33.34**	33.33
jvc_009_001	SPMCS	**30.06**	29.99
NYVTG_006	SPMCS	**33.34**	33.17
HKVTG_004	SPMCS	**29.51**	29.50
veni3_011	SPMCS	36.32	**36.35**
veni5_015	SPMCS	**33.01**	32.99
Foliage	Vid4	26.23	**26.25**
Walk	Vid4	30.66	**30.69**
Calendar	Vid4	**23.93**	23.91
City	Vid4	**27.55**	27.53
Average		**29.35**	29.32

6 CONCLUDING REMARKS

This paper has proposed a novel input frame ranking and selection algorithm for VSR models. The proposed algorithm, STIFS has also revealed the impact of optimal input selection at the architectural level of a learning-based VSR model. It enables VSR neural networks to better learn with spatio-temporal correlation between frames in a given temporal radius of the target frame. Through empirical evaluations on benchmark datasets, the proposed STIFS algorithm has demonstrated its effectiveness over existing sliding window mechanisms. The performance of VSR models can be improved by the proposed STIFS incorporating spatio-temporal metrics in input frame selection. It has demonstrated in the resultant PSNR improvements when using the STIFS algorithm signifies the importance and strong correlation of strategic pixel-aware context-based selection in the input space. The promising results delivered by the STIFS algorithm place it as an adjunct technique that can be adopted in conjunction with any VSR model in order to enhance super-resolution performance while negligible computational effort applies.

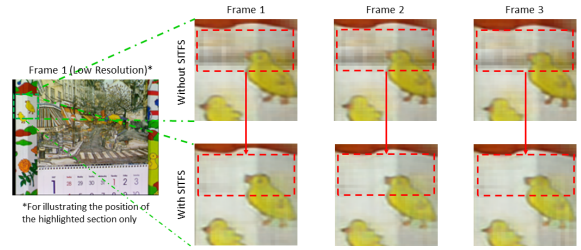

(a) Frames 1, 2 and 3 of Calendar clip

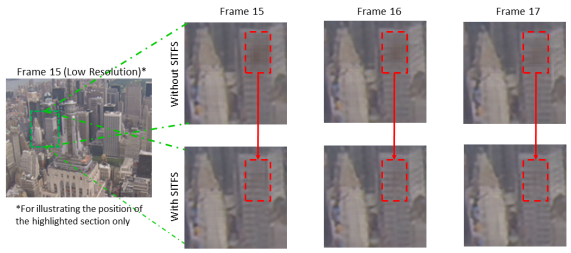

(b) Frames 15, 16 and 17 of City clip

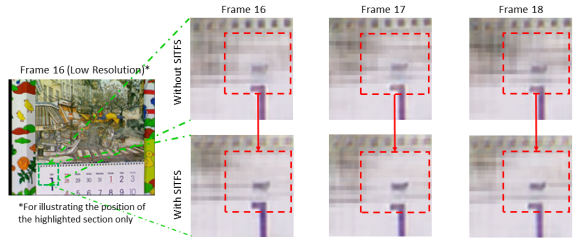

(c) Frames 16, 17 and 18 of Calendar clip

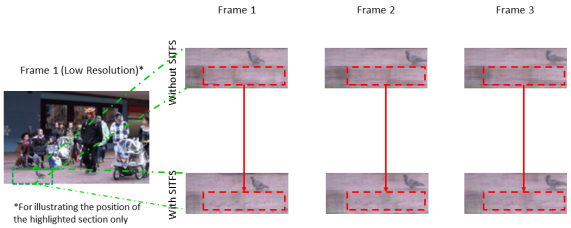

(d) Frames 1, 2 and 3 of Walk clip

Figure 5: Zoomed visual comparison of different frames from various clips of Vid4 dataset. Highlighted red boundary in each frame highlights evident visual quality improvement when using the STIFS algorithm.

REFERENCES

Arefin, M. R., Michalski, V., St-Charles, P.-L., Kalaitzis, A., Kim, S., Kahou, S. E., and Bengio, Y. (2020). Multi-image super-resolution for remote sensing using deep recurrent networks. In *Proceedings of the IEEE/CVF Conference on Computer Vision and Pattern Recognition Workshops*, pages 206–207.

Bao, W., Lai, W.-S., Zhang, X., Gao, Z., and Yang, M.-H. (2021). Memc-net: Motion estimation and motion compensation driven neural network for video interpolation and enhancement. *IEEE Transactions on Pattern Analysis and Machine Intelligence*, 43(3):933–948.

Chan, K. C., Wang, X., Yu, K., Dong, C., and Loy, C. C. (2021). Basicvsr: The search for essential components in video super-resolution and beyond. In *Proceedings of the IEEE/CVF Conference on Computer Vision and Pattern Recognition (CVPR)*, pages 4947–4956.

Dai, J., Qi, H., Xiong, Y., Li, Y., Zhang, G., Hu, H., and Wei, Y. (2017). Deformable convolutional networks. In *Proceedings of the IEEE international conference on computer vision*, pages 764–773.

Haris, M., Shakhnarovich, G., and Ukita, N. (2019). Recurrent back-projection network for video super-resolution. In *Proceedings of the IEEE/CVF Conference on Computer Vision and Pattern Recognition*, pages 3897–3906.

Haris, M., Shakhnarovich, G., and Ukita, N. (2020). Space-time-aware multi-resolution video enhancement. In *Proceedings of the IEEE/CVF Conference on Computer Vision and Pattern Recognition (CVPR)*.

Hung, K.-W., Qiu, C., and Jiang, J. (2019). Video super resolution via deep global-aware network. *IEEE Access*, 7:74711–74720.

Isobe, T., Jia, X., Gu, S., Li, S., Wang, S., and Tian, Q. (2020a). Video super-resolution with recurrent structure-detail network. In Vedaldi, A., Bischof, H., Brox, T., and Frahm, J.-M., editors, *Computer Vision – ECCV 2020*, pages 645–660, Cham. Springer International Publishing.

Isobe, T., Li, S., Jia, X., Yuan, S., Slabaugh, G., Xu, C., Li, Y.-L., Wang, S., and Tian, Q. (2020b). Video super-resolution with temporal group attention. In *Proceedings of the IEEE/CVF Conference on Computer Vision and Pattern Recognition (CVPR)*.

Isobe, T., Zhu, F., Jia, X., and Wang, S. (2020c). Revisiting temporal modeling for video super-resolution. *arXiv preprint arXiv:2008.05765*.

Jo, Y., Oh, S. W., Kang, J., and Kim, S. J. (2018). Deep video super-resolution network using dynamic upsampling filters without explicit motion compensation. In *Proceedings of the IEEE conference on computer vision and pattern recognition*, pages 3224–3232.

Kim, S. Y., Lim, J., Na, T., and Kim, M. (2018). 3dsrnet: Video super-resolution using 3d convolutional neural networks. *arXiv preprint arXiv:1812.09079*.

Liang, M., Du, J., Li, L., Xue, Z., Wang, X., Kou, F., and Wang, X. (2020). Video super-resolution reconstruction based on deep learning and spatio-temporal feature self-similarity. *IEEE Transactions on Knowledge and Data Engineering*, pages 1–1.

Liu, C. and Sun, D. (2013). On bayesian adaptive video su-

per resolution. *IEEE transactions on pattern analysis and machine intelligence*, 36(2):346–360.

Liu, H., Ruan, Z., Zhao, P., Dong, C., Shang, F., Liu, Y., and Yang, L. (2020). Video super resolution based on deep learning: A comprehensive survey. *arXiv preprint arXiv:2007.12928*.

Liu, Z.-S., Siu, W.-C., and Chan, Y.-L. (2021). Efficient video super-resolution via hierarchical temporal residual networks. *IEEE Access*, 9:106049–106064.

Lucas, A., Lopez-Tapia, S., Molina, R., and Katsaggelos, A. K. (2019). Generative adversarial networks and perceptual losses for video super-resolution. *IEEE Trans Image Process*, 28(7):3312–3327.

Nah, S., Baik, S., Hong, S., Moon, G., Son, S., Timofte, R., and Mu Lee, K. (2019). Ntire 2019 challenge on video deblurring and super-resolution: Dataset and study. In *Proceedings of the IEEE/CVF Conference on Computer Vision and Pattern Recognition (CVPR) Workshops*.

Paszke, A., Gross, S., Massa, F., Lerer, A., Bradbury, J., Chanan, G., Killeen, T., Lin, Z., Gimelshein, N., Antiga, L., Desmaison, A., Kopf, A., Yang, E., DeVito, Z., Raison, M., Tejani, A., Chilamkurthy, S., Steiner, B., Fang, L., Bai, J., and Chintala, S. (2019). Pytorch: An imperative style, high-performance deep learning library. In Wallach, H., Larochelle, H., Beygelzimer, A., d'Alché-Buc, F., Fox, E., and Garnett, R., editors, *Advances in Neural Information Processing Systems 32*, pages 8024–8035. Curran Associates, Inc.

Sajjadi, M. S., Vemulapalli, R., and Brown, M. (2018). Frame-recurrent video super-resolution. In *Proceedings of the IEEE Conference on Computer Vision and Pattern Recognition*, pages 6626–6634.

Tao, X., Gao, H., Liao, R., Wang, J., and Jia, J. (2017). Detail-revealing deep video super-resolution. In *Proceedings of the IEEE International Conference on Computer Vision*, pages 4472–4480.

Tian, Y., Zhang, Y., Fu, Y., and Xu, C. (2020). Tdan: Temporally-deformable alignment network for video super-resolution. In *Proceedings of the IEEE/CVF Conference on Computer Vision and Pattern Recognition (CVPR)*.

Wang, H., Su, D., Liu, C., Jin, L., Sun, X., and Peng, X. (2019a). Deformable non-local network for video super-resolution. *IEEE Access*, 7:177734–177744.

Wang, X., Chan, K. C., Yu, K., Dong, C., and Change Loy, C. (2019b). Edvr: Video restoration with enhanced deformable convolutional networks. In *Proceedings of the IEEE/CVF Conference on Computer Vision and Pattern Recognition Workshops*, pages 0–0.

Wang, Z., Chen, J., and Hoi, S. C. (2020). Deep learning for image super-resolution: A survey. *IEEE transactions on pattern analysis and machine intelligence*.

Xue, T., Chen, B., Wu, J., Wei, D., and Freeman, W. T. (2019). Video enhancement with task-oriented flow. *International Journal of Computer Vision*, 127(8):1106–1125.

Zhu, X., Li, Z., Zhang, X.-Y., Li, C., Liu, Y., and Xue, Z. (2019). Residual invertible spatio-temporal network for video super-resolution. In *Proceedings of the AAAI conference on artificial intelligence*, volume 33, pages 5981–5988.